

Partially-reflecting boundary conditions for transient two-phase flow*

Svend Tollak Munkejord[†]

*Norwegian University of Science and Technology (NTNU),
Department of Energy and Process Engineering,
Kolbjørn Hejes veg 1A, NO-7491 Trondheim, Norway*

Abstract

This article deals with partially-reflecting boundary conditions for the four-equation, one-pressure, isentropic two-fluid model. Using PID controllers, this boundary treatment allows waves to pass the boundaries, while keeping the boundary values close to their set-point values, even when the equation system contains source terms.

We consider the water faucet test case. Using the partially-reflecting boundary conditions, the method reaches the correct steady-state solution, and, moreover, in the transient period, the pressure profiles closely resemble the ones produced using non-reflecting boundary conditions.

Keywords: Two-phase flow, Compressible flow, Roe-type method, Characteristic-based boundary conditions, Open boundary conditions

1 Introduction

Physical systems with inlets and outlets, have, unlike the numerical models used to describe them, no abrupt boundaries. Therefore, the numerical boundary conditions may be called artificial, but anyhow, they are required to arrive at a numerical solution.

The specification of open boundaries for flow systems without source terms is relatively straightforward (see e.g. Toro, 1999, Section 6.3.3). However, source terms, such as gravity, often have to be considered. In such cases, the use of the simple, open boundary conditions will most often lead to drifting boundary

*Date: 2005-12-09. Preprint of an article in press in *Communications in Numerical Methods in Engineering*. Copyright © (2005) John Wiley & Sons Ltd.

[†]E-mail: stm@pvv.ntnu.no

values. Hence, for example, one cannot maintain a constant pressure at the outlet boundary.

Here we consider the four-equation, one-pressure, isentropic two-fluid model, assuming both phases to be compressible. Little work has been published regarding open boundary conditions for this system. Indeed, when numerical methods are tested in the literature, the computations are usually halted before the important waves reach the boundaries, to avoid reflected waves interacting with the solution in the inner domain. While that is perfectly justifiable for testing a numerical method, it is not difficult to conceive cases where it would be of interest to conduct longer simulations of the system.

In the present work, we employ the boundary-specification method of Olsen (2004, Chapter 3), who extended the single-phase method of Thompson (1987, 1990) to the two-fluid model, and introduced Proportional-Integral-Derivative (PID) controllers to maintain the boundary quantities close to their desired values. This boundary treatment can be called ‘partially-reflecting’, since a part of the waves reaching the boundary is reflected. The theory of PID controllers can be found in a control-engineering textbook (e.g. Haugen, 1994).

The focus of Olsen (2004) was on essentially stationary cases. The *primary aim* of the present contribution is to demonstrate the applicability of the Olsen method for a transient case. Furthermore, the PID-controller approach involves three parameters. Hence it is our *secondary aim* to give an example of how these parameters can be estimated.

Section 2 briefly describes the two-fluid model formulation, including constitutive relations, while Section 5 reviews the characteristic-based boundary treatment. Numerical tests are performed in Section 6, with the water-faucet case as the main example. Conclusions are drawn in Section 7.

2 Model formulation

This section briefly presents the employed two-fluid model, and the constitutive relations.

2.1 Four-equation system

The one-dimensional, inviscid, isentropic multiphase flow is customarily described by the continuity equation

$$\frac{\partial}{\partial t}(\alpha_k \rho_k) + \frac{\partial}{\partial x}(\alpha_k \rho_k u_k) = 0, \quad (1)$$

and the momentum equation

$$\frac{\partial}{\partial t}(\alpha_k \rho_k u_k) + \frac{\partial}{\partial x}(\alpha_k \rho_k u_k^2) + \alpha_k \frac{\partial p_k}{\partial x} + (p_k - p_{ik}) \frac{\partial \alpha_k}{\partial x} = \alpha_k \rho_k g_x, \quad (2)$$

Table 1: Constants in the equation of state.

	c_k (m/s)	ρ_k° (kg/m ³)
air (g)	$\sqrt{10^5}$	0
water (ℓ)	1000	999.9

when mass transfer, wall friction, interface friction, and other possible effects are neglected. In practical applications, one or more of these effects can be important. In the numerical study presented here, on the other hand, we wish to focus on the mathematically essential parts of the two-fluid model, keeping the number of parameters low.

The following nomenclature is employed: α is the volume fraction, ρ is the density, u is the velocity, g is the acceleration of gravity, p is the phasic pressure and p_i is the interfacial pressure. Here we consider two phases, and the index k can take the values g (gas) and ℓ (liquid). Hence, (1)–(2) represent a system of four equations.

Due to the term $p_{ik}\partial\alpha_k/\partial x$, the equation system cannot be written in conservation form in terms of the variables $\alpha_k\rho_k$ and $\alpha_k\rho_k u_k$.

In addition to the above equations, an equation of state is needed. Here we take

$$p_k = c_k^2(\rho_k - \rho_k^\circ), \quad (3)$$

where the speed of sound, c_k , and the ‘reference density’, ρ_k° , are constants for each phase. In this work we consider air and water, with the properties given in Table 1. These values correspond to the ones used by Evje and Flåtten (2003). The equation of state (3) with constant coefficients is an implicit assumption of isothermal flow. This can be shown using basic thermodynamic relations. As can be seen from Toumi (1996), the entropy waves are advected with the fluid velocities, that is, they are uncoupled from the remaining wave structure, which can therefore be studied by considering an isentropic model.

Moreover, a relation is needed between the pressures in the phases, for example

$$p_k = p_l + \sigma_{kl} \quad \forall k \neq l, \quad (4)$$

where σ_{kl} is a constant pertaining to the relation between the phases k and l . In this work we shall take $\sigma_{kl} = 0$. Finally, of course, a relation for the interfacial pressure p_{ik} must be specified.

The equation system described in this subsection will be called the *four-equation system*.

2.2 Interfacial-pressure model

Several models for the interfacial pressure have been proposed in the literature. However, their physical content is often debatable.

In the CATHARE code, the following expression was employed for non-stratified flows (Bestion, 1990):

$$p_k - p_{ik} = \Delta p_{ik} = \gamma \frac{\alpha_g \alpha_\ell \rho_g \rho_\ell}{\alpha_g \rho_\ell + \alpha_\ell \rho_g} (u_g - u_\ell)^2, \quad (5)$$

where γ is a factor not appearing explicitly in Bestion (1990). It is remarkable that the above expression was employed without physical argumentation, but rather ‘simply to provide the hyperbolicity of the system’, which, indeed, it normally does, at least when there is slip between the phases, that is, $(u_g - u_\ell)^2 \neq 0$. On the other hand, the CATHARE expression has the redeeming feature that it approaches zero in the case of stagnant fluids, which seems reasonable when no surface tension effects are accounted for. Because of this, and because it is commonly cited, the CATHARE model will be used for the interfacial pressure difference, and we will take $\gamma = 1.2$, following Evje and Flåtten (2003).

3 Numerical algorithm

The numerical algorithm employed in the inner domain is described elsewhere, and details may be found by following the references given here.

The governing equations were solved using the wave-propagation (flux-difference splitting) form of Godunov’s method presented by LeVeque (2002, Chapter 15). It is a ‘high-resolution’ method, that is, approaching second order for smooth solutions. The solutions of the Riemann problems at the cell interfaces were found by applying the approximate Riemann solver of Roe (1981) to the two-fluid model (1)–(2). Roe-type methods have been developed for different types of two-phase flow models (Sainsaulieu, 1995; Toumi, 1996; Toumi and Kumbaro, 1996; Karni *et al.*, 2004). The method employed here was of a kind discussed by Evje and Flåtten (2003). Details and discussion of the present numerical method are provided by Munkejord (2005).

To be able to employ the Roe method, we write the system of transport equations in the following quasi-linear form, which will be referred to in Section 5:

$$\frac{\partial \mathbf{q}}{\partial t} + \mathbf{A}(\mathbf{q}) \frac{\partial \mathbf{q}}{\partial x} = \mathbf{s}(\mathbf{q}), \quad (6)$$

with the vector of composite variables

$$\mathbf{q} = \left[\alpha_g \rho_g \quad \alpha_\ell \rho_\ell \quad \alpha_g \rho_g u_g \quad \alpha_\ell \rho_\ell u_\ell \right]^T. \quad (7)$$

The Roe-type method cited above will be called the Roe4 method, since it applies to the four-equation two-fluid model (1)–(2).

4 Steady-state solution

A steady-state solution of the governing equations may, if it exists, be found by carrying out a simulation until the variation in the solution is small enough to be called steady. Another, and computationally far cheaper method, is by making a dedicated steady-state solver. In the present work, this was done by deleting the transient term in (6) and solving the system

$$\frac{d\mathbf{v}}{dx} = \mathbf{B}^{-1}(\mathbf{v})\boldsymbol{\zeta}(\mathbf{v}), \quad (8)$$

where \mathbf{v} is the vector containing the chosen linearly independent primitive variables:

$$\mathbf{v} = [\alpha_g \quad p_g \quad u_g \quad u_\ell]^T, \quad (9)$$

and \mathbf{B} is the coefficient matrix written in terms of \mathbf{v} . $\boldsymbol{\zeta}(\mathbf{v})$ is the vector of source terms. Here we only consider gravity:

$$\boldsymbol{\zeta} = [0 \quad 0 \quad g_x \quad g_x]^T. \quad (10)$$

The system (8) can be solved numerically using a suitable ODE solver if \mathbf{B} is invertible. It is invertible if it has non-zero eigenvalues.

Finding the steady-state solution using this method has advantages due to its efficiency, for instance when one wants to test the effect of interface relations. It is also instructive to test whether transient methods are able to attain the steady-state solution.

5 Characteristic-based boundary treatment

The present boundary treatment is based on the work of Olsen (2004, Chapter 3), who applied the method of Thompson (1987, 1990) to the four-equation system, and introduced a PID controller to specify the conditions at the partially-reflecting boundaries. Here we briefly review the key points of the Olsen approach.

While Olsen (2004) wrote the coefficient matrix \mathbf{A} in terms of the primitive variables \mathbf{v} , here the composite variables \mathbf{q} are employed instead, and this is found to work equally well. This choice is based on practical reasons: The wish to use the same vector of unknowns in the inner domain and at the boundaries.

Since \mathbf{A} is diagonalizable with real eigenvalues, we have:

$$\mathbf{R}^{-1}\mathbf{A}\mathbf{R} = \boldsymbol{\Lambda} = [\lambda_j \delta_{ij}], \quad (11)$$

that is, $\boldsymbol{\Lambda}$ is a diagonal matrix with the eigenvalues of \mathbf{A} along its diagonal.

Multiply the equation (6) by \mathbf{R}^{-1} from the left:

$$\mathbf{R}^{-1} \frac{\partial \mathbf{q}}{\partial t} + \mathbf{R}^{-1} \mathbf{A} \frac{\partial \mathbf{q}}{\partial x} = \mathbf{R}^{-1} \mathbf{s}, \quad (12)$$

and define the vector

$$\mathcal{L} \equiv \Lambda \mathbf{R}^{-1} \frac{\partial \mathbf{q}}{\partial x} \equiv \mathbf{R}^{-1} \mathbf{A} \frac{\partial \mathbf{q}}{\partial x}. \quad (13)$$

Then component j of \mathcal{L} becomes

$$\mathcal{L}_j \equiv \lambda_j \mathbf{l}_j^T \frac{\partial \mathbf{q}}{\partial x}. \quad (14)$$

The equation for the (time dependent) boundary conditions is

$$\frac{\partial \mathbf{q}}{\partial t} + \mathbf{R} \mathcal{L} = \mathbf{s}. \quad (15)$$

We define the vector of characteristic variables, \mathbf{w} , by the relation

$$d\mathbf{w} = \mathbf{R}^{-1} d\mathbf{q}. \quad (16)$$

Using the chain rule, we obtain from (6), neglecting source terms:

$$\frac{\partial \mathbf{q}}{\partial \mathbf{w}} \frac{\partial \mathbf{w}}{\partial t} + \mathbf{A} \frac{\partial \mathbf{q}}{\partial \mathbf{w}} \frac{\partial \mathbf{w}}{\partial x} = \mathbf{0}, \quad (17)$$

Multiply from the left by $\partial \mathbf{w} / \partial \mathbf{q} = \mathbf{R}^{-1}$:

$$\frac{\partial \mathbf{w}}{\partial t} + \Lambda \frac{\partial \mathbf{w}}{\partial x} = \mathbf{0}, \quad (18)$$

or

$$\frac{\partial w_j}{\partial t} + \lambda_j \frac{\partial w_j}{\partial x} = 0 \quad (19)$$

in component form. This is an advection equation for each w_j with λ_j as the characteristic (advection) speed. A system of advection equations represents waves, and λ_j is the wave speed. Therefore, the solution of the nonlinear system (6) consists of several interacting waves.

The interpretation of \mathcal{L} is less obvious, but the equations (18) and (13) show that in the case with no source terms, \mathcal{L} is equal to the negative of the time-derivative of the vector of characteristic variables, \mathbf{w} . Thus \mathcal{L} is related to the time-variation of the wave amplitude. The boundary conditions are therefore specified in terms of \mathcal{L} .

Boundary conditions can only be specified for incoming characteristics. Hence split the boundary-condition equation (15) in the following way:

$$\frac{\partial \mathbf{q}}{\partial t} + \mathbf{R}^+ \mathcal{L}^+ + \mathbf{R}^- \mathcal{L}^- = \mathbf{s}. \quad (20)$$

\mathbf{R}^+ contains the eigenvectors corresponding to the positive eigenvalues (and zero-vectors otherwise), while \mathbf{R}^- does the converse.

Hence, for the *left* boundary, the \mathcal{L}_j^+ s must be specified as boundary conditions, while the \mathcal{L}_j^- s are calculated from the definition (14). Conversely, on the *right* boundary, the \mathcal{L}_j^- s are the boundary conditions, while the \mathcal{L}_j^+ s are calculated from their definition (14).

To specify a function value \mathbf{q}_j at the boundary, one sets $\partial \mathbf{q}_j / \partial t = \mathbf{0}$, so that the equation (20) in component form gives:

$$\mathbf{R}_j^\mp \mathcal{L}^\mp = -\mathbf{R}_j^\pm \mathcal{L}^\pm + \mathbf{s}_j. \quad (21)$$

Here, \mathbf{R}_j denotes row j of \mathbf{R} .

It is also possible to specify a spatial gradient. The equation (13) implies that

$$(\mathbf{A}^{-1} \mathbf{R})_j \mathcal{L} = \frac{\partial \mathbf{q}_j}{\partial x} \quad (22)$$

or

$$(\mathbf{A}^{-1} \mathbf{R}^\mp)_j \mathcal{L}^\mp = \frac{\partial \mathbf{q}_j}{\partial x} - (\mathbf{A}^{-1} \mathbf{R}^\pm)_j \mathcal{L}^\pm. \quad (23)$$

Non-reflecting boundaries are set by specifying $\mathcal{L}^\mp \equiv \mathbf{0}$. However, in several cases with non-zero source terms, this may lead to ‘drifting’, or undetermined, values at the boundaries (Olsen, 2004, Section 3.3).

Drifting values can be avoided by making the boundaries partially-reflecting. A good way of doing that, is by thinking of the boundary treatment in terms of PID controllers (Olsen, 2004, Chapter 3). Hence write

$$\mathbf{R}_j^\mp \mathcal{L}^\mp = (\mathbf{R}_j^\mp \mathcal{L}^\mp)^\circ + \frac{k_P}{T} \Delta \mathbf{q}_j + \frac{k_I}{T^2} \int_0^t \Delta \mathbf{q}_j d\tau + k_D \frac{\partial \mathbf{q}_j}{\partial t}. \quad (24)$$

Herein, $(\mathbf{R}_j^\mp \mathcal{L}^\mp)^\circ$ is a start term. If the initial conditions are ‘good’, a suitable value for the start term is $-\mathbf{R}_j^\pm \mathcal{L}^\pm + \mathbf{s}_j$. $\Delta \mathbf{q}_j = \mathbf{q}_j - \mathbf{q}_j^{\text{ref}}$ is the discrepancy between the desired value $\mathbf{q}_j^{\text{ref}}$ and the actual one. k_P , k_I and k_D are the proportional, integral and differential constants, respectively. T is an integral time scale.

Substitute $\partial \mathbf{q}_j / \partial t$ in (24) by using the equation (20) in component form:

$$\frac{\partial \mathbf{q}_j}{\partial t} = -\mathbf{R}_j^\pm \mathcal{L}^\pm - \mathbf{R}_j^\mp \mathcal{L}^\mp + \mathbf{s}_j. \quad (25)$$

This gives:

$$\mathbf{R}_j^\mp \mathcal{L}^\mp = (1 + k_D)^{-1} [(\mathbf{R}_j^\mp \mathcal{L}^\mp)^\circ + \frac{k_P}{T} \Delta \mathbf{q}_j + \frac{k_I}{T^2} \int_0^t \Delta \mathbf{q}_j d\tau - k_D (\mathbf{R}_j^\pm \mathcal{L}^\pm - \mathbf{s}_j)]. \quad (26)$$

Using the above equations for the boundary conditions is here, as in Olsen (2004), referred to as the MPCBC (multiphase characteristic-based boundary conditions) method.

6 Numerical tests

We have chosen the water faucet of Ransom (1987) as a test case for the multiphase characteristic-based boundary conditions (MPCBC). Since gravity is included, simply setting $\mathcal{L}^\mp \equiv \mathbf{0}$ would not work for specifying open boundary conditions, as that would cause a drifting outlet pressure. Hence the approach of the equation (26) is needed.

The results shown in the following have been calculated using the monotonized central-difference (MC) limiter function. The resulting numerical scheme approaches second order when the solution is smooth. Details and calculations regarding limiter functions, and convergence order of the scheme, can be found in Munkejord (2005).

6.1 Problem description

The water faucet case is described in Ransom (1987), and it has become a common test case for one-dimensional two-fluid models. The problem consists of a vertical tube 12 m in length and 1 m in diameter. Here, of course, it is represented one-dimensionally. A schematic is shown in Figure 1 on the following page. The top has a fixed volumetric inflow rate of water at a velocity of $u_\ell^\circ = 10$ m/s, a liquid volume fraction of $\alpha_\ell^\circ = 0.8$, and a temperature of $T = 50$ °C. The bottom of the tube is open to the ambient pressure, $p = 1.0 \cdot 10^5$ Pa, and the top of the tube is closed to vapour flow.

Initially, the flow is uniform throughout the computational domain, and the initial conditions are equal to the inlet conditions. A thinning of the liquid jet will take place due to the effect of gravity.

6.2 Analytical expressions for volume fraction and velocity

Ransom (1987) stated that when pressure variation in the vapour phase is ignored, the transient problem has a simple analytical solution. Coquel *et al.* (1997)

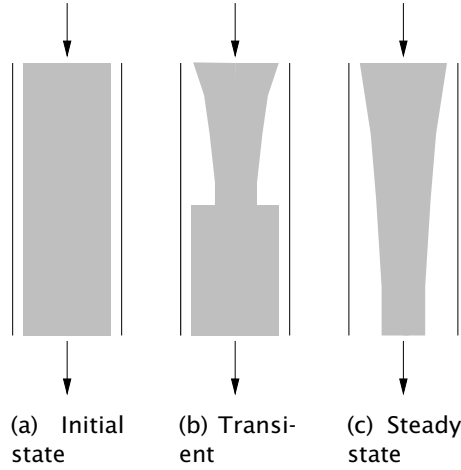


Figure 1: Sketch of the water faucet test case. In the transient phase, a volume-fraction discontinuity propagates towards the exit.

provided the solution for the gas volume-fraction profile:

$$\alpha_g(x, t) = \begin{cases} 1 - \frac{\alpha_\ell^\circ u_\ell^\circ}{\sqrt{2gx + (u_\ell^\circ)^2}} & \text{if } x \leq u_\ell^\circ t + \frac{1}{2}gt^2, \\ 1 - \alpha_\ell^\circ & \text{otherwise,} \end{cases} \quad (27)$$

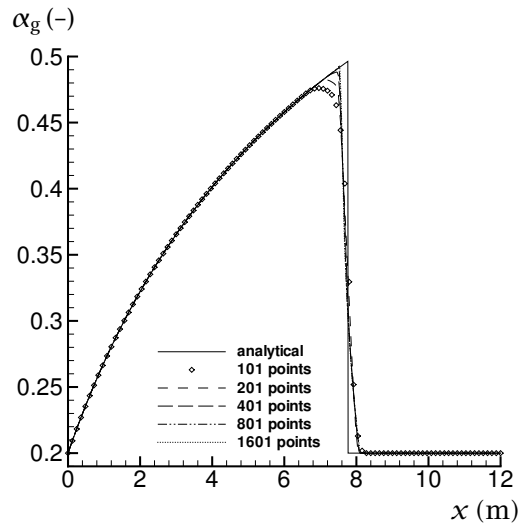
and the expression for the liquid velocity is given by Evje and Flåtten (2003):

$$u_\ell(x, t) = \begin{cases} \sqrt{(u_\ell^\circ)^2 + 2gx} & \text{if } x \leq u_\ell^\circ t + \frac{1}{2}gt^2, \\ u_\ell^\circ + gt & \text{otherwise.} \end{cases} \quad (28)$$

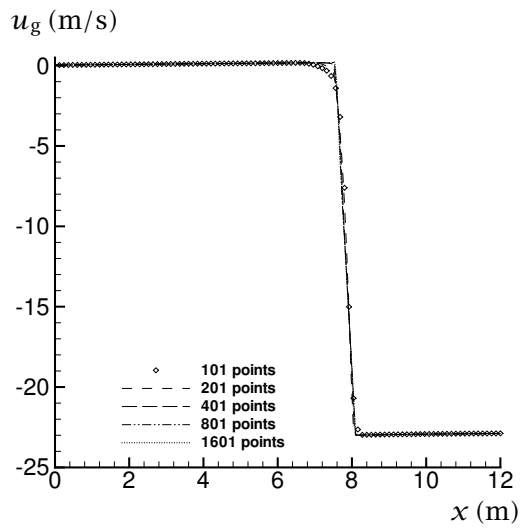
A partial description of the solution procedure can be found in Trapp and Riemke (1986).

6.3 Grid convergence

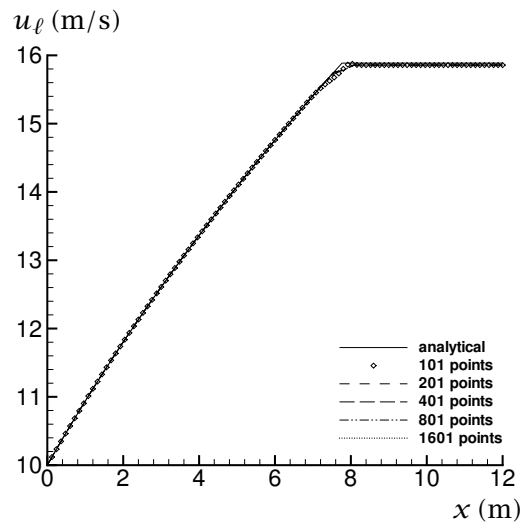
The grid convergence of the Roe4 method was tested on numerical grids ranging from 101 to 1601 grid points. The time step was set to $\Delta t = 1.97 \cdot 10^{-5}$ s, which corresponds to a Courant–Friedrichs–Lewy (CFL) number of $C = 0.9$ for the finest grid. This is shown in Figure 2 on the next page for the volume fraction, and the gas and liquid velocities. For the volume fraction and the liquid velocities, where analytical expressions are available, good correspondence is obtained, but the convergence is less than second order. This is due to the discontinuity in the solution. For discontinuous solutions, the smooth-solution order of the scheme can normally not be attained (see LeVeque, 2002, Section 8.7).



(a) Gas volume fraction



(b) Gas velocity



(c) Liquid velocity

Figure 2: Water faucet. Grid convergence of the Roe4 method.

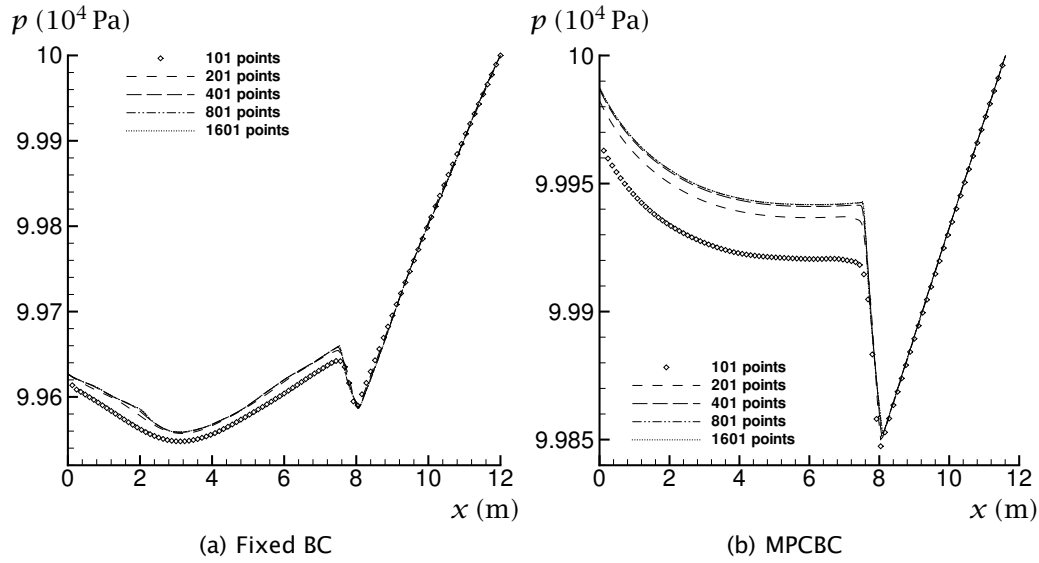


Figure 3: Pressure for the water faucet. Grid convergence of the Roe4 method for fixed and characteristic-based boundary conditions (MPCBC).

6.3.1 Pressure

The pressure is by far the most sensitive variable in the faucet case. It is shown in Figure 3 for the for simple, fixed boundary conditions, and MPCBC. It can be observed that the solution is quite different, depending on how the boundary conditions are specified. The fixed boundary conditions employed in Figure 3(a) give a larger pressure difference across the computational domain than the MPCBC method shown in Figure 3(b). This is further discussed in the following.

For the volume fraction and the velocities, on the other hand, the effect of the boundary treatment is not obvious until the volume-fraction discontinuity reaches the outlet.

6.4 Estimation of controller parameters

Recall the equation (26) on page 8 for the PID-controller boundary condition. It is necessary to estimate some reasonable values for the controller parameters appearing there. Here, this was done by using a slightly modified version of the closed-loop method by Ziegler and Nichols (1942) as presented in the control-engineering textbook by Haugen (1994, Section 7.3).

In the present work, we assign the value $T = 1$ s for the time scale in the equation (26), which is sufficient, since we shall not discuss the controller-parameter values and the time scale independently. Assume that the 'critical

gain', k_c , and the corresponding 'critical period', T_c , can be estimated. Then the Ziegler-Nichols method corresponds to setting

$$k_P = 0.6k_c, \quad k_I = \frac{2k_P T_c}{T_c}, \quad \text{and} \quad k_D = \frac{k_P T_c}{8T_c}, \quad (29)$$

where k_P , k_I and k_D , are defined by the equation (26).

The pressure, p , was used as the 'control variable' for determining k_P , k_I , and k_D . In normal control theory, the critical gain, k_c , is determined by setting k_I and k_D equal to zero and increasing the gain (corresponding to k_P) until the appearance of standing waves. Here, however, it is not the pressure, p , that is controlled, but its time derivative. Hence a steady state could not be attained without the integral term, and the proportional term was found instead by trial and error.

The period T_c was estimated by setting reasonably good 'trial-and-error' values for the controller parameters, and then measuring the period of the pressure fluctuations at the outlet. Values of $k_P = 300$, $k_I = 650$ and $k_D = 0$ were taken. This gave a value for the period of $T_c \approx 0.18$ s. The period was only a weak function of the controller parameters in this region.

Setting $k_P = 150$ gave, using $T_c = 0.18$ s, $k_I = 1667$ and $k_D = 3.3$. These values gave satisfactory results, that is, not too large initial fluctuations, and small fluctuations in the steady state. Doubling and halving k_P was also tried, calculating the corresponding k_I and k_D using $T_c = 0.18$ s each time. However, $k_P = 300$ gave unacceptably large fluctuations in the 'steady' state, and $k_P = 75$ gave rather large initial fluctuations. Hence, $k_P = 150$ was found to be a good compromise and retained for all the faucet-case calculations by the Roe4 method.

The above method for determining the controller parameters is undoubtedly improvable, but, as will be demonstrated in the following, it did indeed give reasonable results.

6.5 Influence of boundary-condition 'reflectiveness'

Consider Figure 4 on the following page. It is similar to Figure 3 on the previous page, but instead of grid refinement, it shows the dependence on the choice of boundary conditions on the inlet and the outlet. The label pairs shown in the figure, for instance 'fixed,PID', indicate the boundary conditions on the left-hand and on the right-hand sides, respectively. 'PID' means that the boundary conditions are set using the equation (26), while 'fixed' indicates that the equation (21) is used, that is, that the boundaries are reflecting. 'Open' means that the \mathcal{L}_j s are set to zero for incoming characteristics.

When the outlet boundary condition is 'open' (the \boxminus curve), the pressure will drop. Hence the curve for the open outlet condition is drawn using the right-hand ordinate. The other curves relate to the left-hand ordinate. Both ordinates have

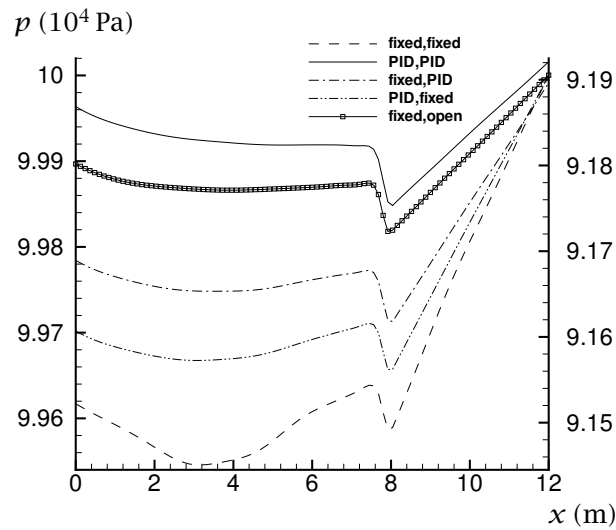


Figure 4: Pressure for the water faucet. Dependence on choice of inlet and outlet boundary conditions. The ‘fixed,open’ curve is related to the right-hand ordinate.

the same span of 480 Pa, and the right-hand ordinate has been set such that the outlet pressure corresponds to $10 \cdot 10^4$ Pa on the left-hand ordinate.

The boundary-specification method giving by far the lowest pressure change across the domain, at the particular time of $t = 0.6$ s, was the use of PID controllers at both boundaries. The use of fixed boundary conditions produced the largest pressure changes at the inlet. When an open boundary was set at the outlet, it did not matter whether the inlet condition was fixed or PID.

Among the different combinations of reflecting and partially-reflecting boundary conditions, the one with a PID controller at both ends was the one that gave a pressure profile that best matched the shape of the profile calculated using the open boundary condition at the outlet. This shows that for the faucet case, the PID-controller boundary conditions succeeded in

- Keeping the outlet pressure from deviating too far from the set-point pressure of $1.0 \cdot 10^5$ Pa, and
- Giving results closely resembling those obtained using open boundary conditions at the outlet.

For the volume fraction and the liquid velocity, all the boundary conditions gave virtually the same result. Regarding the gas velocity, however, there were some differences, as shown in Figure 5 on the following page. The three combinations of PID conditions gave very similar gas-velocity profiles, whereas the most negative

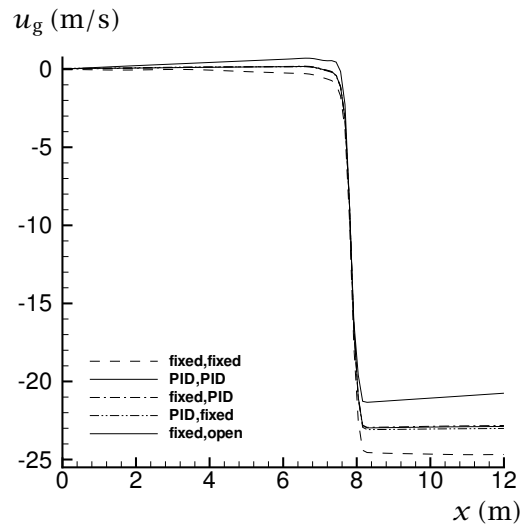


Figure 5: Gas velocity for the water faucet. Dependence on choice of inlet and outlet boundary conditions.

velocity occurred for the fixed inlet–fixed outlet condition, and the least negative velocity was calculated using the open-outlet condition.

The difference in pressure arising from the use of PID or fixed boundary conditions is further illustrated in Figure 6. In Figure 6(a), a PID controller has been used at both boundaries, and in Figure 6(b), fixed conditions were employed. As can be seen, the amplitude of the pressure fluctuation at the inlet is about three times larger in the case of fixed boundary conditions compared to PID-controller conditions. Hence, if the pressure is important in itself, or if one wants, for instance, to calculate mass transfer due to flashing, a proper choice of boundary conditions is of significance.

6.6 Calculations towards steady state

The steady-state solution of the faucet case was calculated by two different methods:

1. By carrying out simulations with the Roe4 method until $t = 3$ s, and
2. By solving the steady-state system (8) on page 5 using a standard ODE solver.

Again the pressure was the most sensitive variable, and the result is displayed in Figure 7 on the following page. For Figure 7(a), the Roe4 method was run using PID controllers at both boundaries. At $t = 3$ s, the correspondence between the

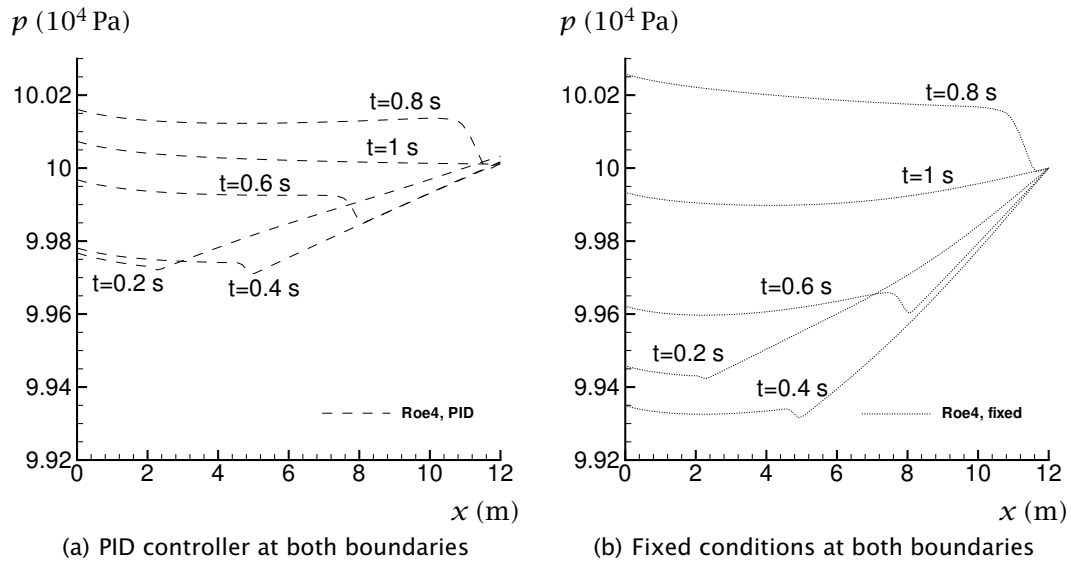


Figure 6: Pressure for the water faucet. Time series showing the influence of boundary conditions.

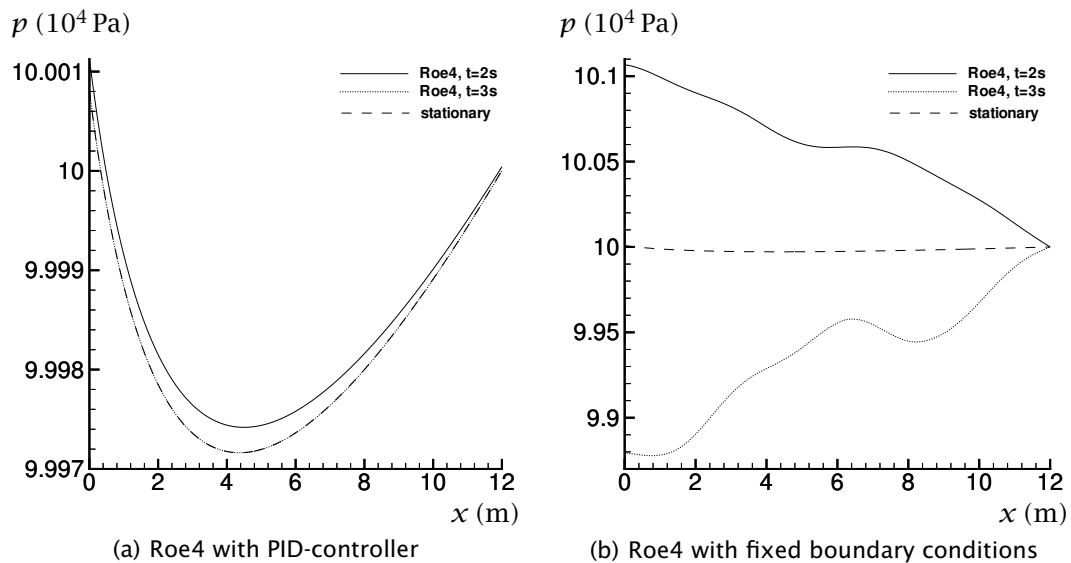


Figure 7: Pressure for the water faucet. Comparison of steady-state solution as obtained with the Roe4 solver with and without PID-controller boundary conditions, and with the stationary solver.

Roe4 solution and the stationary solution is very good, and this result is not obtained by chance: Using a non-PID boundary condition at any boundary would lead to the Roe4 method utterly failing to produce the stationary pressure profile. This is shown in Figure 7(b). Note that the scale of the ordinate is different; in Figure 7(b), the shown pressure interval is 2400 Pa, while it is 41.25 Pa in Figure 7(a).

The pressure profiles obtained in Figure 7(a) are different from the linear shape one would expect in a case where gravity is the only source term. In fact, this is a result of the use of the CATHARE correlation (5) for the interfacial pressure difference. Indeed, when calculations were performed with a vanishing interfacial pressure difference, the pressure profile approached a linear shape. Physically, this can be explained by considering the liquid falling in stagnant air. The air is stagnant, and it will have a hydrostatic pressure profile. At the same time, it is reasonable that the air and water have the same pressure at each cross section, since no surface tension or other effects causing different phasic pressures are present.

Remark Another question is how the pressure calculated using different boundary conditions would compare with the pressure in the physical system for which the faucet case is a simplified model. Furthermore, as can be seen from the equation (14), the \mathcal{L}_j s are proportional to the left eigenvectors, which are not unique. Hence, the transient behaviour at a PID-controlled boundary is dependent on the choice of eigenvectors as well as on the controller parameters. These are two interesting issues for further studies.

7 Conclusions

For compressible flow, the specification of open boundary conditions is non-straightforward when the system of equations contains source terms, because they can cause drifting boundary values.

In this work, we have studied the one-dimensional one-pressure two-fluid model, solving it using a Roe-type method. The multiphase characteristic-based boundary condition (MPCBC) method of Olsen (2004) was employed. It uses PID controllers at the boundaries to avoid drifting values, while keeping the solution close to the desired set-point values.

We have aimed to demonstrate that the MPCBC method is applicable to transient cases. Furthermore, we have illustrated how the PID-controller parameters can be estimated. With the water-faucet case of Ransom (1987) as an example, it has been shown that MPCBC can yield a reasonable approximation to physically ‘open’ boundary conditions. Specifically, during the transient period, the MPCBC method gave a pressure profile closely resembling that of open boundary conditions, and

the correct steady-state solution was attained. The pressure profile obtained using fixed boundary conditions was noticeably different from that obtained using PID controllers at the boundaries.

It is believed that the MPCBC method can be used for the simulation of systems with open boundaries, even after important waves have reached the boundaries.

Acknowledgements

I am grateful to have received a doctoral fellowship from the Research Council of Norway.

I would like to thank my colleague Robert Olsen for letting me use his numerical code as a starting point for implementing the method tested in the present work.

Thanks are due to the referees for their constructive remarks on the first version of this paper. The comments of Erik B. Hansen and Robert Olsen on the manuscript are also acknowledged.

References

- Bestion, D. The physical closure laws in the CATHARE code. *Nuclear Engineering and Design*, volume 124, no. 3: pages 229-245, December 1990.
- Coquel, F., El Amine, K., Godlewski, E., Perthame, B. and Rascle, P. A numerical method using upwind schemes for the resolution of two-phase flows. *Journal of Computational Physics*, volume 136, no. 2: pages 272-288, 1997.
- Evje, S. and Flåtten, T. Hybrid flux-splitting schemes for a common two-fluid model. *Journal of Computational Physics*, volume 192, no. 1: pages 175-210, November 2003.
- Haugen, F. *Regulering av dynamiske systemer*. Tapir Forlag, Trondheim, Norway, 1994. ISBN 82-519-1433-7.
- Karni, S., Kirr, E., Kurganov, A. and Petrova, G. Compressible two-phase flows by central and upwind schemes. *ESAIM: Mathematical Modelling and Numerical Analysis*, volume 38, no. 3: pages 477-493, May-June 2004.
- LeVeque, R. J. *Finite Volume Methods for Hyperbolic Problems*. Cambridge University Press, Cambridge, UK, 2002. ISBN 0-521-00924-3.
- Munkejord, S. T. *Analysis of the two-fluid model and the drift-flux model for numerical calculation of two-phase flow*. Doctoral thesis, Norwegian University of Science and Technology, Department of Energy and Process Engineering, Trondheim, November 2005. ISBN 82-471-7338-7.

- Olsen, R. *Time-dependent boundary conditions for multiphase flow*. Doctoral thesis, Norwegian University of Science and Technology, Department of Energy and Process Engineering, Trondheim, September 2004. ISBN 82-471-6313-4.
- Ransom, V. H. Faucet flow. In: G. F. Hewitt, J. M. Delhay and N. Zuber, editors, *Numerical Benchmark Tests*, volume 3 of *Multiphase Science and Technology*, pages 465–467. Hemisphere/Springer, Washington, USA, 1987. ISBN 0-89116-561-4.
- Roe, P. L. Approximate Riemann solvers, parameter vectors, and difference schemes. *Journal of Computational Physics*, volume 43, no. 2: pages 357–372, October 1981.
- Sainsaulieu, L. Finite-volume approximation of two phase-fluid flows based on an approximate Roe-type Riemann solver. *Journal of Computational Physics*, volume 121, no. 1: pages 1–28, October 1995.
- Thompson, K. W. Time-dependent boundary conditions for hyperbolic systems. *Journal of Computational Physics*, volume 68, no. 1: pages 1–24, January 1987.
- Thompson, K. W. Time-dependent boundary conditions for hyperbolic systems, II. *Journal of Computational Physics*, volume 89, no. 2: pages 439–461, August 1990.
- Toro, E. F. *Riemann solvers and numerical methods for fluid dynamics*. Springer-Verlag, Berlin, second edition, 1999. ISBN 3-540-65966-8.
- Toumi, I. An upwind numerical method for two-fluid two-phase flow models. *Nuclear Science and Engineering*, volume 123, no. 2: pages 147–168, 1996.
- Toumi, I. and Kumbaro, A. An approximate linearized Riemann solver for a two-fluid model. *Journal of Computational Physics*, volume 124, no. 2: pages 286–300, March 1996.
- Trapp, J. A. and Riemke, R. A. A nearly-implicit hydrodynamic numerical scheme for two-phase flows. *Journal of Computational Physics*, volume 66, no. 1: pages 62–82, September 1986.
- Ziegler, J. G. and Nichols, N. B. Optimum settings for automatic controllers. *Transactions of the ASME*, volume 64: pages 759–768, 1942.